Journal of Computer Engineering
ISSN 10003428

Original Research Article
Vol 12, Issue 6, 2023 | ISSN: 1000-3428

A Novel Approach to Turbomachinery Blading Design in Three-Dimensional Flow Using Commercial CFD Tools

Mohammad Ali Rostami, Ali Reza Mirzaei

Department of Aerospace Engineering, University of Toronto; Centre for Engineering in Medicine, Massachusetts General Hospital

Abstract

An aerodynamic inverse shape design of turbomachinery blading in three-dimensional viscous flow is developed and implemented into a commercial CFD program, namely ANSYS-CFX. It is applied to redesign the rotor blades of an axial compressor stage and an axial turbine stage.

Indexed keywords: Computer Engineering, Advanced Computing, Technology, Open Access

Article History: Received: 06 March 2023 | Accepted: 08 May 2023 | Published: 02 June 2023

The design method is based on specifying one blade parameter, the stacking line (a blade line from hub to tip), and two other parameters such as the blade loading and thickness distribution or the pressure distributions on blade surfaces. This inverse design approach is fully consistent with the viscous flow assumption and is independent of the CFD approach taken.

An axial compressor stage E/CO-3 and turbine stage E/TU-3 are analysed and the results thus obtained are assessed against available experimental data. These stages are then inversely designed in order to improve their aerodynamic performance.

INTRODUCTION

Inverse design methods date back several decades and were first implemented on two-dimensional potential flow, then for inviscid flow and finally viscous flow. Due to this evolution, most of the inverse approaches used today still have some traces of the inviscid flow that might affect the scheme stability or consistency.

[Giles and Drela, (1987)] [1] made use of viscous-inviscid interaction and [Damle *et al, (1999)*] [2] used the tangency condition to compute the designed blade camber-line. In other methods such as [Demeulenaere *et al.,* (1997)] [3], the transpiration condition has been used where the tangential and normal components of the velocity on the blade are computed to find the new blade profile. Another approach, [de Vito *et al.,* (2003)] [4], uses both Navier Stokes and Euler solvers for the flow analysis and inverse design, respectively; or the work done by [Mendes *et al.,* (2009)] [5] which used artificial viscosity to take the viscous effects into account. In all of these methods it has been assumed that the flow is attached to the blade and the boundary layer is well behaved. In the other word, in cases where flow separation occurs, these methods are questionable and reliable results may not be obtained. In most inverse methods neither the mesh movement is accounted for in the computations nor the transient term is considered so that the solution is transposed from one mesh to the next and the problem is solved as quasi-steady (time marching) problem; such as the methods surveyed and classified by Dulikravich [6].

There are however a few inverse design methods which are based on the difference between the instantaneous and prescribed (fixed) target pressure distribution that use RANS or Unsteady RANS (URANS) formulation for the design implementation. For example the work by [Hield *et al.,* (2008)] [7] who used the time marching form of RANS equations in 3D flow which was later on extended to the inverse design of 3D fan blades at dual operating points where the algorithm is developed as a stand-alone code [8]; another example is the method of [Mileshin, (2007)] [9] which is developed into an in-house code and uses the time accurate formulations to design a full 3D transonic fan rotor. Similarly the method of [Daneshkhah and Ghaly, (2006); Daneshkhah and Ghaly, (2007)] [10], [11] who used the time accurate formulation for the design in two-dimensional flow and modified the governing equations to account for the mesh movement. The latter approach was later on implemented by [Arbabi and Ghaly, (2013)] [12] into a commercial CFD program where for the first time the same CFD code was used for both analysing as well as designing the blade profile into a shape which satisfies a given design target e.g. the loading or static pressure distribution.

The current research builds on the work of [Arbabi and Ghaly, (2013)] [12] who implemented into ANSYS-CFX the inverse design method originally developed by Daneshkhah and Ghaly and used it for the redesign of compressor and turbine blades in two-dimensional flow.

The 2D method is extended to the redesign of blades in three-dimensional flow and is then implemented into ANSYSCFX using the tools provided by ANSYS to interact with the CFD program. The design variables used in the

How to cite: Mohammad Ali Rostami, Ali Reza Mirzaei (2023). A Novel Approach to Turbomachinery Blading Design in Three-Dimensional Flow Using Commercial CFD Tools. Journal of Computer Engineering, 12(6), 77–84. DOI: https://doi.org/10.5281/zenodo.19349290

present work are either static pressure on the blade pressure or suction surfaces or the pressure loading and the blade thickness. The validation of the methodology was presented in the recent work of [Arbabi *et al.*, (2017)] [13] and this paper covers its implementation on axial compressor and turbine blades to assess the design robustness and to measure how accurately the prescribed target is satisfied; the design intent being to improve the stage performance.

This study also demonstrates that the present inverse method can be coupled to, and is independent of, the CFD flow solver used.

Methodology

The design method assumes the blade wall to be moving with a virtual velocity that is computed based on the difference between the current (or instantaneous) and the target (or fixed) pressure distributions. The blade deforms repeatedly in order to satisfy the prescribed target function. As the instantaneous pressure on the blade surface gets closer to the target, the virtual velocity diminishes accordingly and asymptotes to zero upon satisfaction of the target pressure. The nodes located on the blade surface move, based on the virtual velocity, to a new position to shape a new blade profile which produces the prescribed target.

The resulting blade is scaled back to the original chord length. The discrete points are interpolated back to their original axial location, thereby the span-wise blade sections are essentially moving only in the tangential direction normal to the blade shape. The new normal camber-line of all designed airfoils are then computed and smoothed out. The prescribed normal thickness corresponding to each discrete point is added to the camber-line and the designed 3D blade surface is reconstructed.

The resulting blade displacement is returned to CFX which computes the mesh motion for the rest of the domain so as to match the new blade profile while maintaining the mesh quality. The flow field is then computed over the new blade and the design is advanced to the next time-step; the process is repeated until the target is reached within some tolerance.

The details of the inverse design formulations, constraints and algorithm are published in [Arbabi *et al.*, (2017)] [13].

Results and Discussion

Analysis of the E/CO-3 Compressor Stage

The single stage subsonic compressor, called E/CO-3, was selected and first analysed in ANSYS-CFX at two operating points on the design speed line (of 9,262.5 rpm) namely Maximum Flow and Design conditions.

Mesh sensitivity study was performed at maximum flow conditions on two different meshes using two different turbulence models (K-Omega, BSL) where for the fine mesh there are 1.17m nodes on the rotor and 680k nodes on the stator, while for the coarse mesh there are 760k nodes on the rotor and 440k nodes on the stator blades. Boundary layer is resolved with more than 15 mesh lines for both meshes as shown in figure 1.

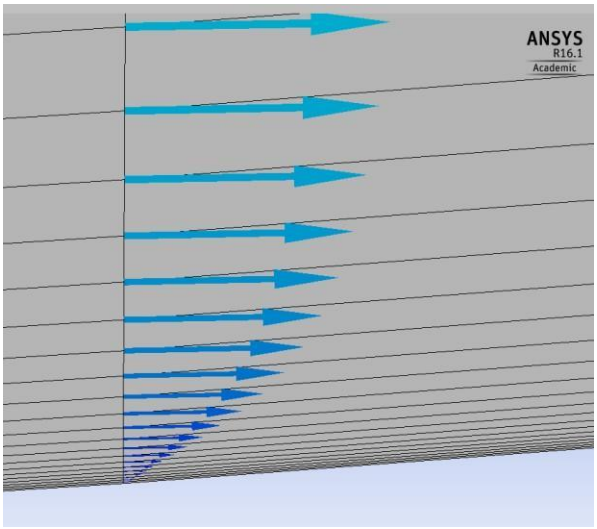

Figure 1. Velocity profile inside the boundary layer of the fine mesh

The results were then compared against the experimental data [Fottner, 1990] [14] which are given in Table 1 and it was observed that the computed and measured data match very well with a discrepancy below 1% for most of the flow parameters. As the results obtained for both turbulence models were almost identical, the flow parameters corresponding to the BSL model only is provided in the table. The E/CO-3 stage was then analysed at design conditions. Based on the observations in mesh sensitivity study at maximum flow where the fine and coarse mesh results matched reasonably, for the design point the analysis is carried out using the coarse mesh and BSL turbulence model and the results thus obtained were compared with experimental data as listed in Table 2. Small discrepancies were observed for some of the flow parameters such as exit total pressure for which two reasons could be the cause: One is the small change in the stage back pressure (2 kPa or about 2% of the experimental back pressure) to obtain the mass flow rate and stage pressure ratio as close as possible to the experimental **Table 1. E/CO-3 compressor stage analysis results at Maximum Flow**

	measured	Coarse mesh	Fine mesh
Inlet P_0 (kPa)	95.7	95.57	95.48
Stage PR	1.196	1.193	1.194
Efficiency (%)	85.7	85.71	86.1
Exit Mach	0.419	0.419	0.419
TRR	0.0612	0.0605	0.0605
$\dot{m}$ (kg/s)	9.9	9.89	9.89
Exit flow angle	-1.5	-1.99	-1.95
Exit T_0 (K)	305.62	305.41	305.43
Exit P_0 (kPa)	115	114.03	114.04

data. The second reason is the geometry itself which may be slightly different from the real geometry. To construct the geometry used in this research, the raw data available in [Fottner, 1990] [14] has been used through which b-spline curves [Piegl, (1997)] [15] are fitted to obtain the airfoils at different span-wise sections. However, the discrepancy does not exceed 2.5% at worst.

Table 2. E/CO-3 compressor stage analysis results at Design Point

	measured	Computed
Inlet P_0 (kPa)	95.0	95.3
Inlet T_0 (K)	288	288
Stage PR	1.236	1.233
Efficiency (%)	88.3	89.6
Exit Mach	0.375	0.385
TRR	0.0707	0.0690
$\dot{m}$ (kg/s)	9.4	9.5
Exit flow angle	1.1	2.0
Exit T_0 (K)	308.35	307.849
Exit P_0 (kPa)	119.4	117.6

Redesign of the E/CO-3 compressor stage at Maximum Flow

The inverse design method was then applied to the redesign of the E/CO-3 compressor stage. The rotor was redesigned first at maximum flow conditions; while the stator blade shape was fixed. This is obtained by running ANSYSCFX for the stage with one row running in inverse mode while the other is running in analysis mode.

The design intent was to increase the total-to-total efficiency of the stage by specifying a target loading pressure distribution that would correspond to a lower negative incidence on the rotor as well as lower peak Mach number on the blade suction surface compared with the original blade so as to reduce the diffusion and the chance of flow separation.

The blade is consisted of 30 span-wise airfoils with 294 nodes on each. 6 span-wise grids located at the hub, 15%, 40%, 60%, 85% and 98% span were selected to be designed and the remaining sections between 0-98% of blade height are obtained by interpolation and Morphing method [Guan *et al., (2014)*] [16]. The rotor blade has tip clearance hence the last 2% of the blade (in span-wise direction) is obtained by extrapolation. This is done because the flow uncertainties and the adverse span-wise pressure gradient caused by the tip clearance, makes the design at those sections extremely difficult, if not impossible.

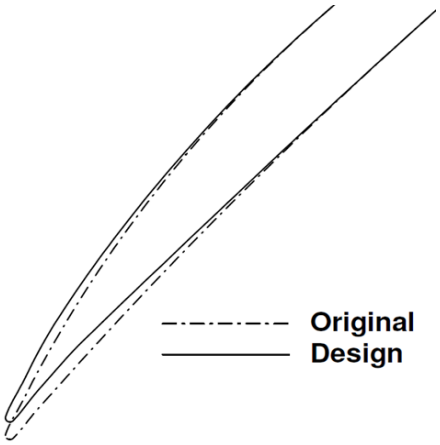

a.15% span geometry

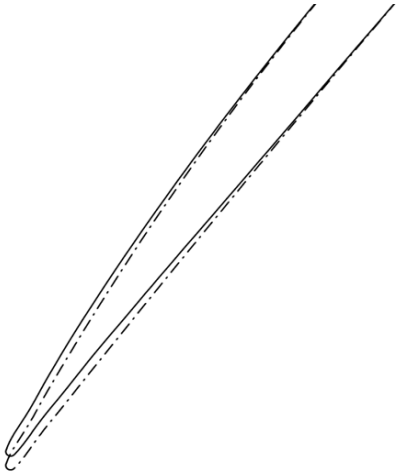

b. 60% span geometry

b.60% span geometry

Figure 2. E/CO-3 Rotor Redesign: Original and designed geometry at 15% & 60% span

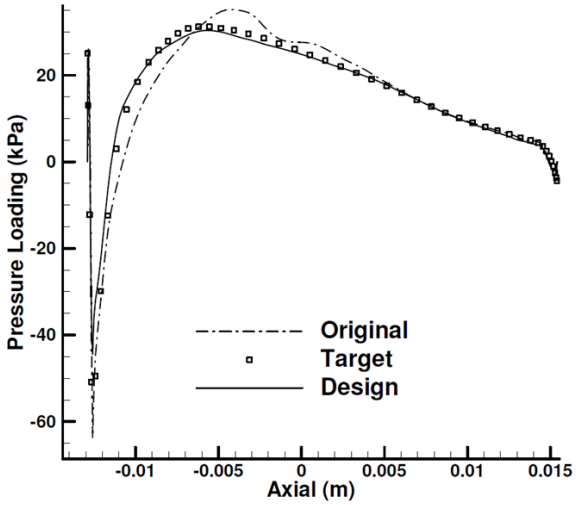

a. 15% span loading

a.15% span loading

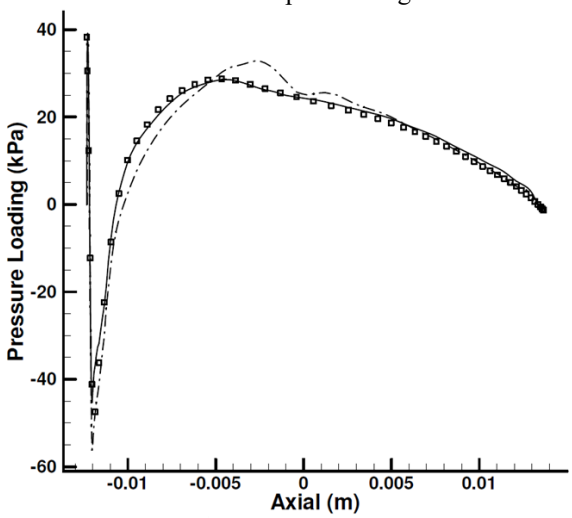

b.60% span loading

Figure 3. E/CO-3 Rotor Redesign: Original, target and designed pressure loading at 15% & 60% span

The design took 70 steps (approximately equivalent to one flow simulation) to satisfy the prescribed target loading by about 80%. Figures 2 and 3 show the original and design airfoils geometry and pressure loading at 15% and 60% span.

By analysing the flow around the new blade it was observed that the peak Mach number over the suction surface as well as the adverse pressure gradient are reduced which leads to a reduced diffusion and consequently a reduction in the stage pressure loss. Moreover the negative incidence at rotor inlet has also been reduced. These factors combined led to an increase of 0.8% in total-to-total stage efficiency. Table 3 compares flow parameters before and after the design.

Redesign of the E/CO-3 compressor stage at Design Point

The method was then applied to the redesign of the rotor blade at design conditions. For this purpose, the stage designed at maximum flow was first analysed at design conditions and the new loading thus obtained (preliminary target) was used to generate the final target loading that corresponds to a further reduced negative incidence and adverse pressure gradient by shifting the peak loading upstream towards the LE.

Table 3: Original and design flow parameters at maximum flow conditions

	Original	Design
Stage PR	1.193	1.196
Efficiency (%)	85.71	86.50
Exit Mach	0.419	0.424
TRR	0.0605	0.0608
Exit flow angle	-1.99	-1.95
Exit T_0 (K)	305.41	305.52
Exit P_0 (kPa)	114.03	114.33

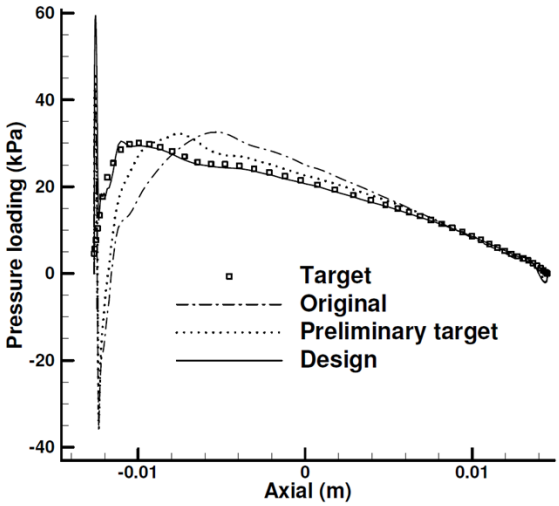

a.40% span loading

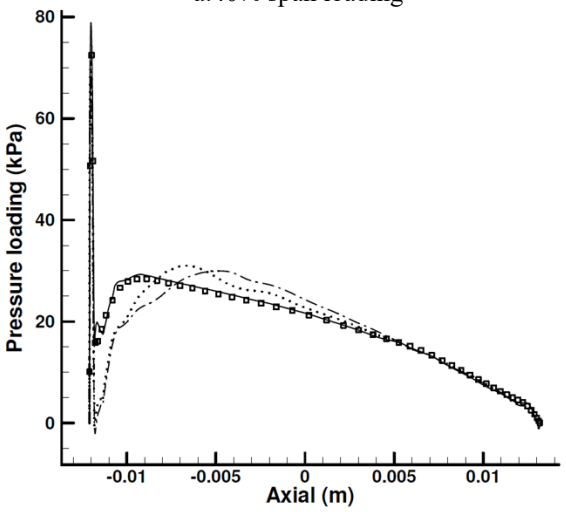

b.85% span loading

Figure 4. E/CO-3 Rotor redesign at Design Point:

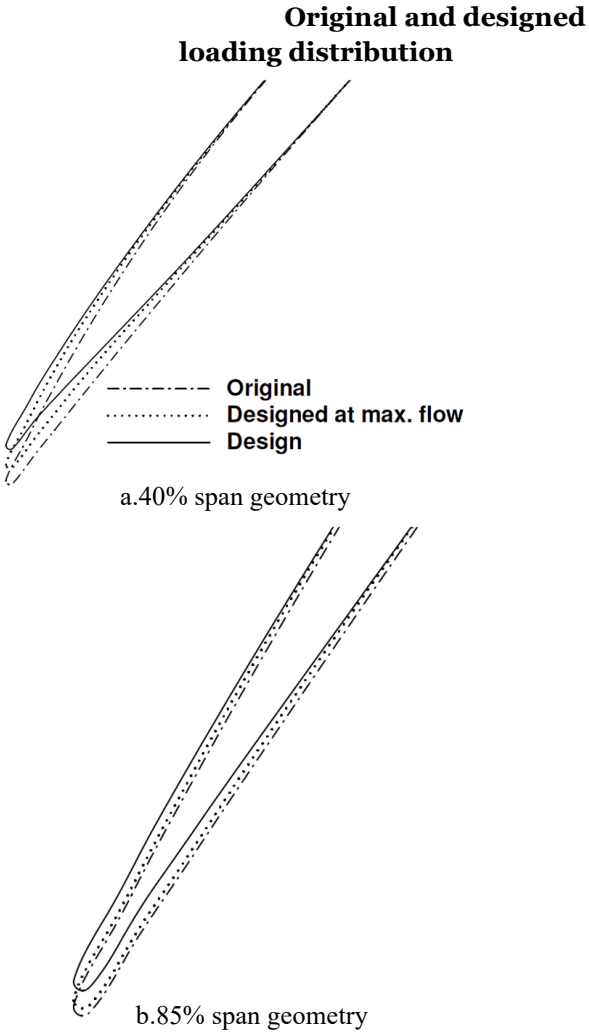

Figure 5. E/CO-3 Rotor redesign at Design Point: Original and designed airfoils

After 130 design steps the negative incidence was reduced until complete elimination. The pressure gradient as well as the peak Mach number on the suction surface were further reduced which resulted in about 0.5% of efficiency improvement at design point.

Figures 4, 5 and 6 respectively compare the loading, geometry and the static pressure of the original bale, the blade designed at maximum flow and the blade designed at design conditions at 40% and 85% span. Table 4 summarizes the flow parameters at design point and compares them with the original stage. It could be seen from figure 4 that the peak loading is pushed further upstream and the negative incidence is reduced until complete elimination as the minimum loading near the LE does not reach a negative value. Figure 6 also confirms the previous statement where for the design case (solid line) the pressure of suction and pressure surfaces do not cross each other at the LE.

The designed stage was then analysed at maximum flow conditions and the results were compared with the first design at maximum flow conditions expecting a better performance. In fact the achievement was beyond the expectations. Table 5 gives the flow parameters for both design cases and compares them with the original stage. Figures 7 and 8 show the original and design loading and pressure distributions.

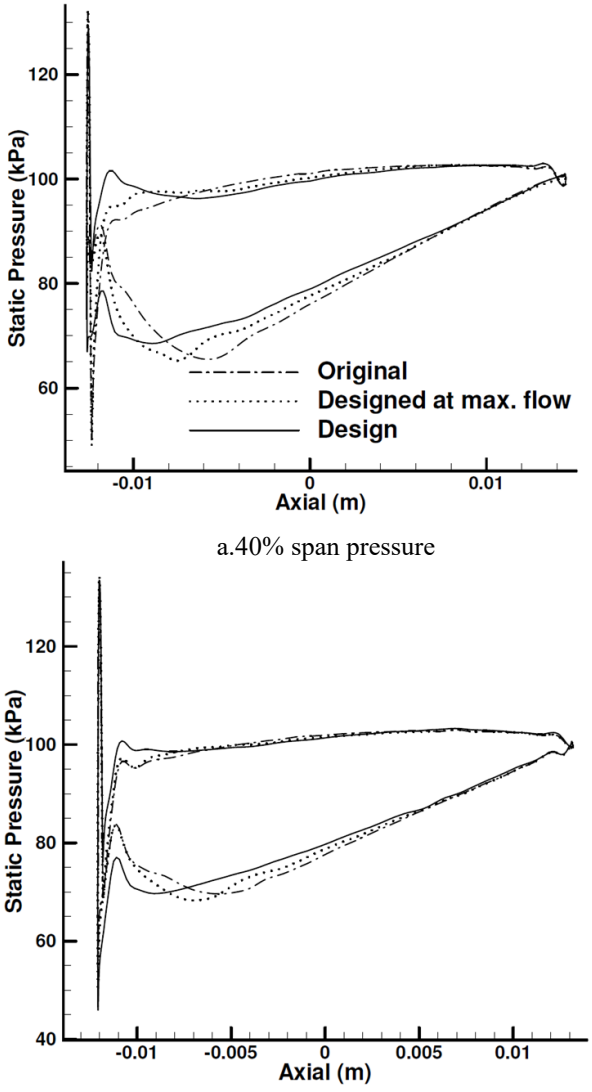

Figure 6. E/CO -3 Rotor redesign at Design Point: Original and designed static pressure

Table 4. Original and design flow parameters at Design Point

	Original	Design
Stage PR	1.233	1.236

Efficiency (%)	89.6	90.05
Exit Mach	0.385	0.390
TRR	0.0690	0.0693
Exit flow angle	2.0	2.0
Exit T_0 (K)	307.849	307.97
Exit P_0 (kPa)	117.6	117.88

Table 5. Original and design flow parameters at Maximum Flow

	Original	1st Design	2nd Design
Stage PR	1.193	1.196	1.199
Efficiency (%)	85.71	86.50	87.6
Exit Mach	0.419	0.424	0.427
TRR	0.0605	0.0608	0.0607
Exit flow angle	-1.99	-1.95	-1.92
Exit T_0 (K)	305.41	305.52	305.51
Exit P_0 (kPa)	114.03	114.33	114.56

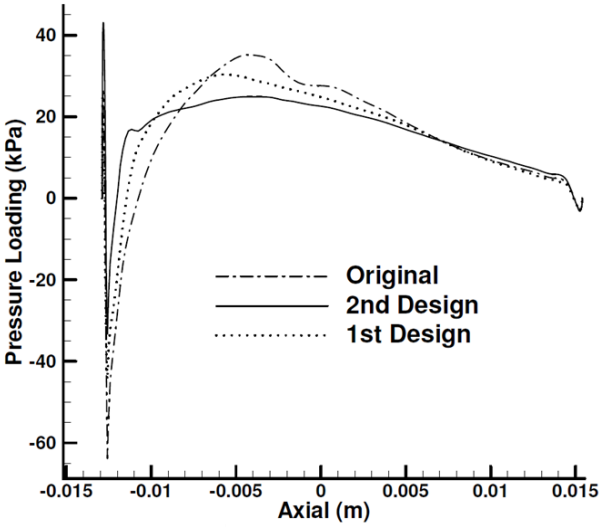

a.15% span loading

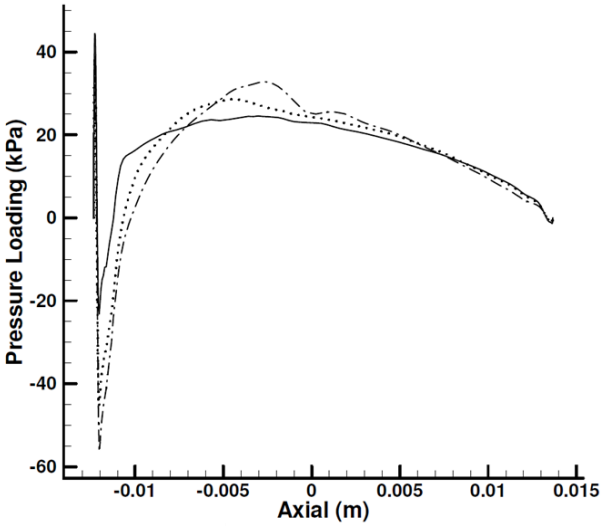

b.60% span loading

Figure 7. E/CO-3 Rotor redesign at Maximum Flow: Original and designed loading distribution

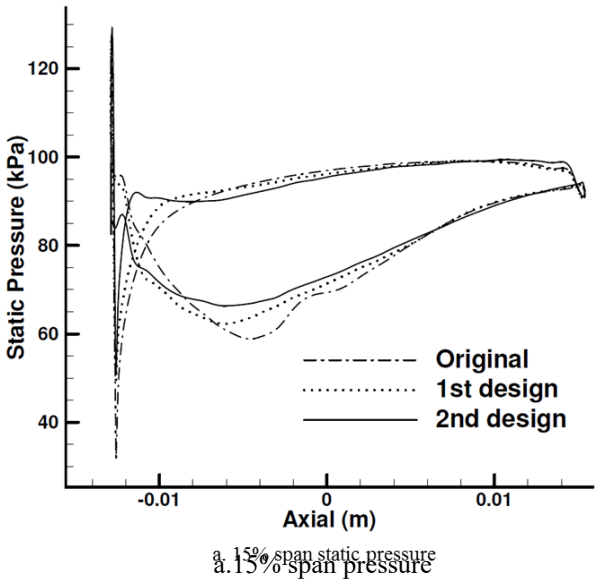

a. 15% span static pressure

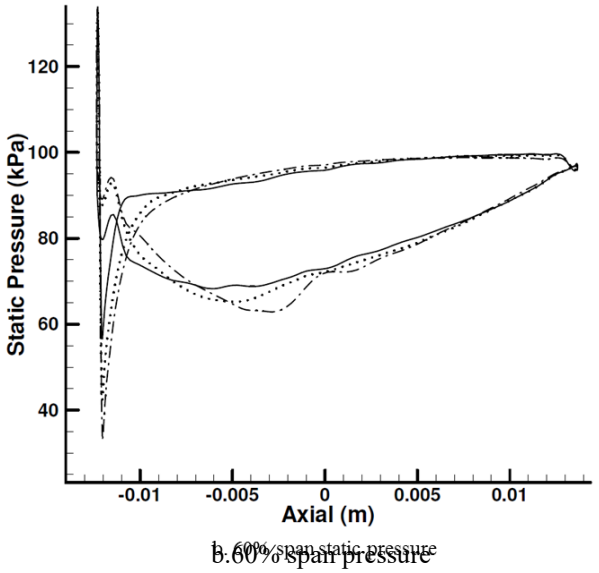

b. 60% span static pressure

Figure 8. E/CO-3 Rotor redesign at Maximum Flow: Original and designed static pressure

It can be seen that both negative incidence and peak Mach number as well as the adverse pressure gradient on the suction surface are significantly reduced resulting in a considerable improvement of 1.9% in total to total efficiency of the stage at maximum flow conditions.

The span-wise efficiency and stream-wise pressure gradient of the rotor blade for the original and both design cases at maximum flow conditions are shown in figures 9 and 10. The significant reduction of the pressure gradient around the midchord and improvement of the efficiency all the way from hub to tip could be seen in these figures.

Analysis of the E/TU-3 Turbine Stage

The low speed axial turbine stage E/TU-3 was analysed in ANSYS-CFX at design point on the design speed line of 7800 rpm [Fottner, 1990] [14].

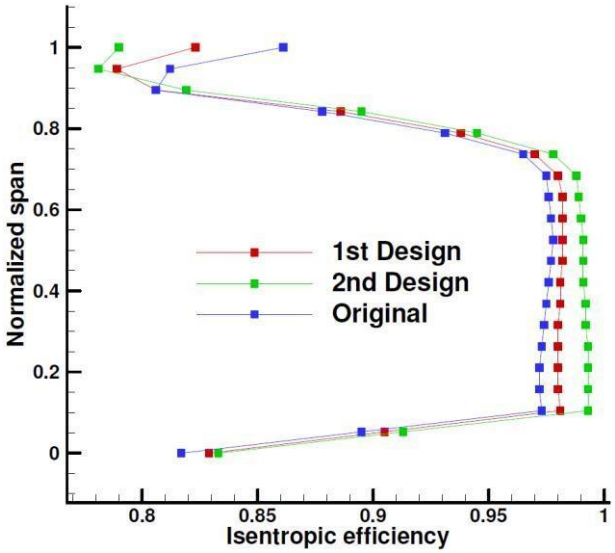

Figure 9. E/CO-3 Rotor: Original and designed efficiency in span-wise direction

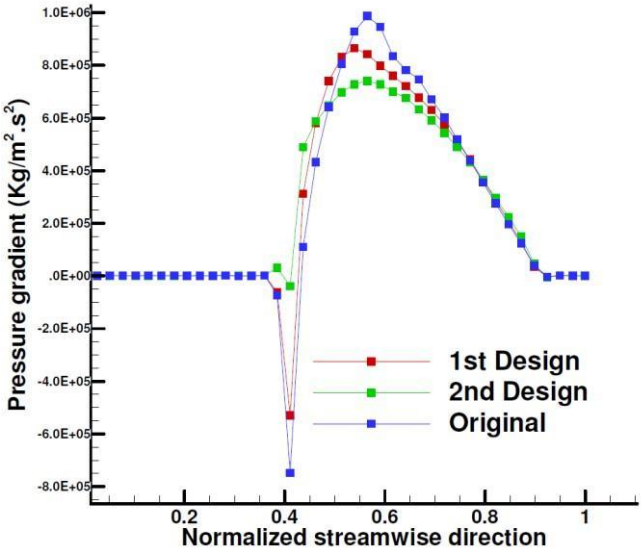

An O-Grid mesh is constructed around the blade to resolve the boundary layer; the rest of the domain is filled with structured mesh by using the so-called "Automatic ATM Optimized topology" setting available in TurboGrid. The rotor and stator domains contained 303K and 316K nodes, respectively. The analysis results are given in Table 6. The discrepancy between the computed results and the experimental data were found to be below 1.5% at worst.

Redesign of the E/TU-3 turbine stage at Design Point

The inverse method was then used to redesign the turbine rotor while the stator is fixed and under analysis only. In addition to the reduction of the peak Mach number on suction surface, the overall loading was slightly increased (by 3%) in order to increase the stage reaction which was expected to have positive impact on the stage efficiency.

The design variables were the blade pressure loading and normal thickness distributions and the stacking line which was set at the LE. The rotor blade consists of 38 airfoils in the span- wise direction with 214 nodes on each. Six span-wise airfoils

Figure 10. E/CO-3 Rotor: Original and designed pressure gradient in stream-wise direction

Table 6. E/TU-3 turbine stage analysis results at Design Point

	measured	computed
Stage PR	0.57	0.57
Reduced $\dot{m}$ (kg.k/s.bar)	97	97.7
Efficiency (%)	89.6	89.8
Exit T_0 (K)	300	299.6
Enthalpy drop (j/kg.k)	132	134
Rotor inlet flow angle	44.7	44.4
Stator exit flow angle	68.3	68.5

Journal of Computer Engineering
ISSN 10003428
Original Research Article
Vol 12, Issue 6, 2023 | ISSN: 1000-3428

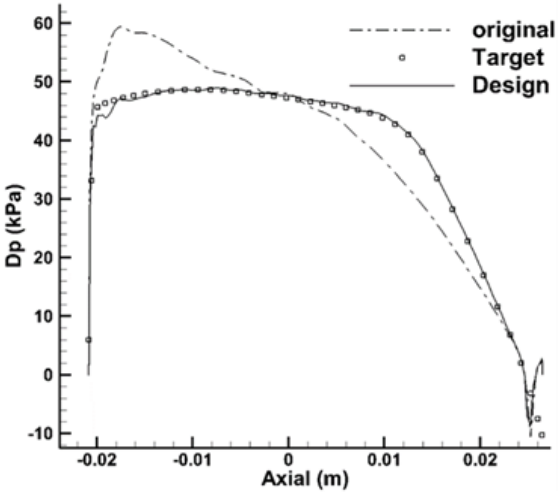

a.55% span loading

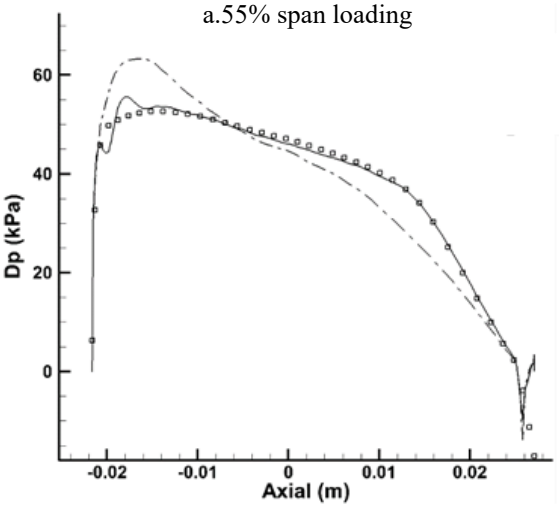

b.80% span loading

Figure 11. E/TU-3 Rotor redesign: Original, target and design loading at 55% and 80%

How to cite: Mohammad Ali Rostami, Ali Reza Mirzaei (2023). A Novel Approach to Turbomachinery Blading Design in Three-Dimensional Flow Using Commercial CFD Tools. Journal of Computer Engineering, 12(6), 77–84. DOI: https://doi.org/10.5281/zenodo.19349290

Journal of Computer Engineering
ISSN 10003428
Original Research Article
Vol 12, Issue 6, 2023 | ISSN: 1000-3428

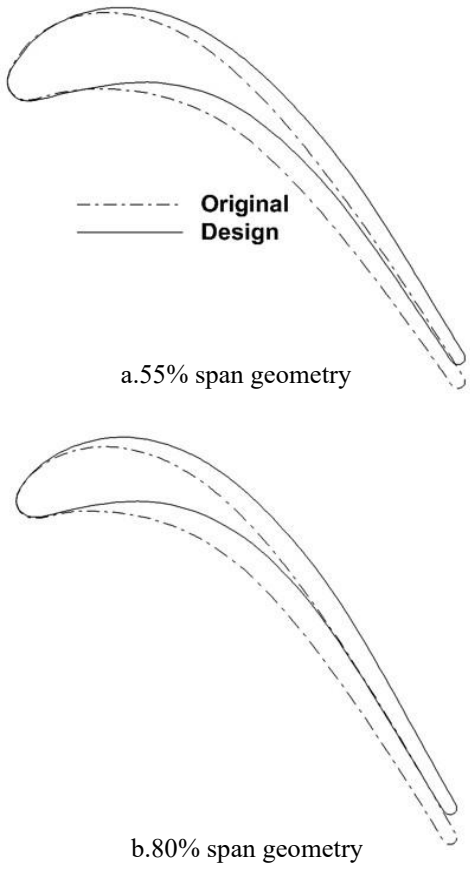

a.55% span geometry

b.80% span geometry

Figure 12. E/TU-3 Rotor redesign: Original and design geometry at 55% and 80% span

located at the rotor hub, 17%, 35%, 55%, 80% and the rotor tip section were chosen as the design airfoils for which a target pressure loading was generated. The remaining airfoils were then obtained by Morphing method.

The first and last 5% of the airfoils were run in analysis mode to ensure that the blade shape is closed and smooth while the non-designed LE/TE potions in compressor blades is 2-3% chord. The reason is the larger thickness of turbine blades where the LE/TE circles cover around 5% of the chord which is aimed to be left outside the design region. The inverse design converged in 150 design steps in total.

The design process was interrupted a few times and the designed blade (at that stage of the design) was run in analysis mode so as to remove any accumulated flow unsteadiness during the transient run. The design process was then continued from the latest obtained designed blade. At the end of design process the prescribed target loading was satisfied by 80% on average. The design results are listed in Table 7. Figures 11, 12 and 13 show the original and design loading, airfoil geometry and static pressure at 55% and 80% span.

The reduction of the peak loading and peak Mack number on suction surface could be clearly seen from figures 13. The modified blade shape (figure 12) also shows that the maximum camber at about 10% chord is reduced and shifted downstream the blade which resulted to loading gain at midchord.

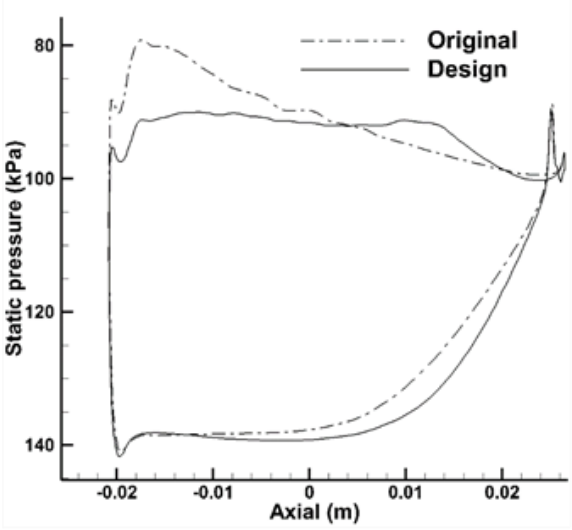

a.55% span pressure

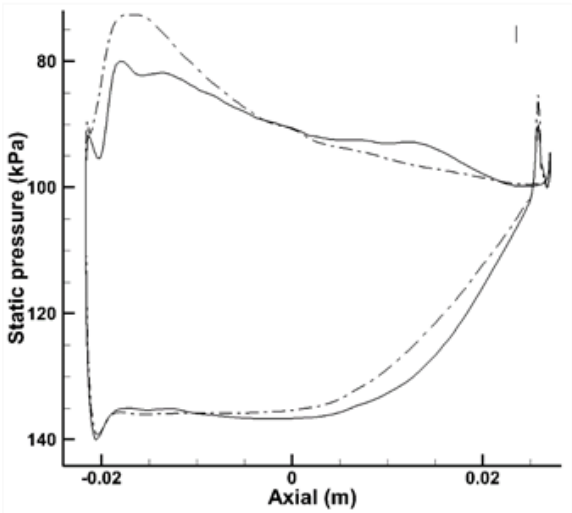

b.80% span pressure

Figure 13. E/TU-3 Rotor redesign: Original and design static pressure at 55% and 80%

Table 7. E/TU-3 turbine stage: Original and design flow parameters

	Original	Design
Efficiency (%)	89.8	90.2

How to cite: Mohammad Ali Rostami, Ali Reza Mirzaei (2023). A Novel Approach to Turbomachinery Blading Design in Three-Dimensional Flow Using Commercial CFD Tools. Journal of Computer Engineering, 12(6), 77–84. DOI: https://doi.org/10.5281/zenodo.19349290

Enthalpy drop (j/kg.k)	134	135
Stage PR	0.57	0.57
Reduced $\dot{m}$ (kg.k/s.bar)	97.7	97.6
Exit T_0 (K)	299.6	299.4
Rotor exit flow angle	-53.03	-53.67
Mach at exit	0.656	0.663
Stage reaction (%)	31	33

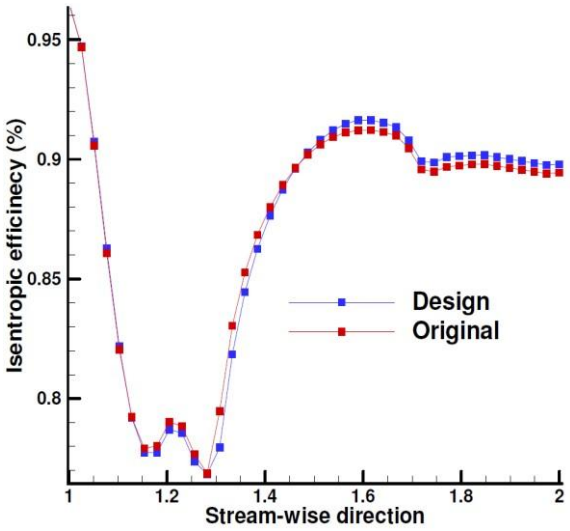

Figure 14. E/TU-3 Rotor: Original and designed efficiency in stream-wise direction

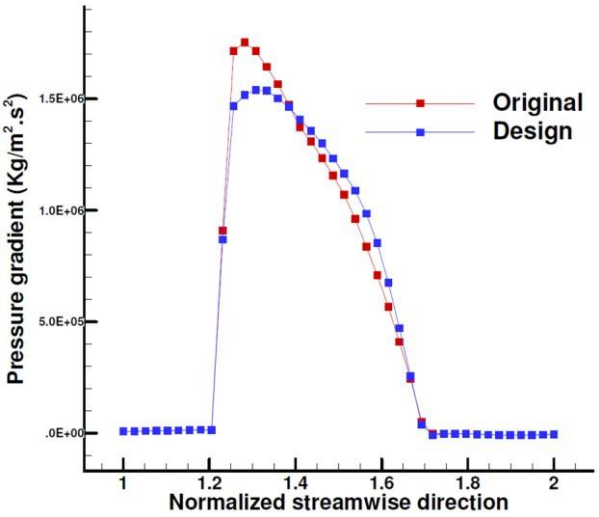

Figure 15. E/TU-3 Rotor: Original and designed pressure gradient in stream-wise direction

The slight loading gain has also caused the increase in stage reaction by 2% and all the mentioned modifications led to an increase of 0.4% in stage total to total efficiency.

The stream-wise efficiency and adverse pressure gradient of the original and designed rotor blade at design point are shown in figures 14 and 15. Although the performance is a bit suffered at the first 30% chord due to the loading loss at that area (figures 11 and 13), the reduction of adverse pressure gradient and suction surface Mach number at mid-chord as well as the loading gain at downstream region improved the overall performance.

Conclusion

An aerodynamic inverse shape design method has been developed and successfully implemented into a commercial CFD program in the context of axial compressors and turbines. The method, which is fully consistent with viscous flow, was applied to the redesign of a subsonic compressor stage and a low speed turbine stage which resulted in improvement of 0.5% to 2% for the compressor and 0.4% for the turbine stage. This work demonstrates the ability to inverse-design turbomachinery stages using the same CFD code used in analyzing them. Combined with an established CFD program the method becomes available for the designers in the field who can take advantage of all its features and save a huge amount of time and effort to develop a 3D solver from scratch.

REFERENCES

[1] M. Giles and M. Drela, "Two-dimensional transonic aerodynamic design method," *AIAA,* vol. 25, pp. 11991205, 1987.

[2] S. Damle, T. Dang, J. Stringham and E. Razinsky, "Practical use of a 3d viscous inverse method for the design of compressor blade," *Journal of Turbomachinery,* vol. 121, no. 2, pp. 321-325, 1999.

[3] A. Demeulenaere, O. Leonard and R. Van den Braembussche, "A two-dimensional navier-stokes inverse solver for compressor and turbine blade design," *Proceedings of the Institution of*

Mechanical Engineers, PART A., 211, pp. 299-307, 1997.

[4] L. de Vito, R. V. den Braembussche and M. Deconinck, "A novel two-dimensional viscous inverse design method for turbomachinery blading," *Journal of Turbomachinery,* vol. 125, pp. 310-316, 2003. [5] J. P´ascoa, A. C. Mendes and L. M. C. Gato, "A Fast Iterative Inverse Method for Turbomachinery Blade," *Mechanics Research Communications,* vol. 36, no. 5, p. 630–637, 2009.

[6] G. S. Dulikravich, "Aerodynamic shape design and optimization: Status and trends," *Journal of Aircraft,* vol. 29, no. 6, pp. 1020-1026, 1992.

[7] P. Hield, "Semi-Inverse Design Applied to an Eight Stage Transonic Axial Flow Compressor," in *Proceedings of ASME Turbo Expo, GT2008-50430*, 2008.

[8] J. H. Page, P. Hield and P. G. Tucker, "Inverse Design of 3D Multi-Stage Transonic Fans at Dual Operating Points," in *Proceedings of ASME Turbo Expo, GT201395062*, 2013.

[9] V. Mileshin, I. Orekhov, S. Shchipin and A. Startsev, "3D Inverse Design of Transonic Fan Rotors Efficient for a Wide Range of RPM," in *Proceedings of ASME Trubo Expo - GT2007-27817*, 2007.

[10] K. Daneshkhah and W. Ghaly, "An inverse blade design method for subsonic and transonic viscous flow in compressors and turbines," *Journal of Inverse Problems in Science and Engineering,* vol. 14, no. 3, pp. 211-231, 2006.

[11] K. Daneshkhah and W. Ghaly, "Aerodynamic inverse design for viscous flow in turbomachinery blading," *AIAA Journal of Propulsion and Power,* vol. 23, no. 4, pp. 814-820, 2007.

[12] A. Arbabi and W. Ghaly, "Inverse Design of Turbine and Compressor Stages Using a Commercial CFD Program," in *Proceedings of ASME Turbo Expo - GT2013-96017*, San Antonio, 2013.

[13] A. Arbabi and W. Ghaly, "Aerodynamic Inverse Blade Design of Axial Compressors in Three-Dimensional Flow Using a Commercial CFD Program," in *Proceedings of ASME Turbo Expo - GT2017-65194*, Charlotte, 2017.

[14] L. Fottner, "Test cases for computation of internal flows in aero engine components," *AGARD-AR-275,* 1990.

[15] L. Piegl and W. Tiller, The Nurbs Book, Springer, 1997.

[16] L. Gaun, D. Bestle and A. Huppertz, "Hot-To-Cold CAD Geometry Transformation of Aero Engine Parts Based on B-Spline Morphing," in *Proceedings of the ASME Turbo Expo 2014.*, 2014.